

Suppression of rotating machine shaft-line torsional vibrations by a driving asynchronous motor using two advanced control methods

Paweł HAŃCZUR^{1,2}, Tomasz SZOLC¹, and Robert KONOWROCKI¹

¹ Institute of Fundamental Technological Research of the Polish Academy of Sciences, ul. Pawińskiego 5B, 02-106 Warsaw, Poland

² Schneider Electric Polska Sp. z o.o, ul. Konstruktorska 12, 02-673 Warsaw, Poland

Abstract. Many industrial rotating machines driven by asynchronous motors are often affected by detrimental torsional vibrations. In this paper, a method of attenuation of torsional vibrations in such objects is proposed. Here, an asynchronous motor under proper control can simultaneously operate as a source of drive and actuator. Namely, by means of the proper control of motor operation, it is possible to suppress torsional vibrations in the object under study. Using this approach, both transient and steady-state torsional vibrations of the rotating machine drive system can be effectively attenuated, and its precise operational motions can be assured. The theoretical investigations are conducted by means of a structural mechanical model of the drive system and an advanced circuit model of the asynchronous motor controlled using two methods: the direct torque control – space vector modulation (DTC-SVM) and the rotational velocity-controlled torque (RVCT) based on the momentary rotational velocity of the driven machine working tool. From the obtained results it follows that by means of the RVCT technique steady-state torsional vibrations induced harmonically and transient torsional vibrations excited by switching various types of control on and off can be suppressed as effectively as using the advanced vector method DTC-SVM.

Key words: rotating machine; drive system; asynchronous motor; torsional vibrations; control methods.

1. INTRODUCTION

From among various kinds of vibrations occurring in drive systems of machines, and vehicles, the torsional ones are very important as naturally associated with their fundamental rotational motion. Torsional vibrations are a source of additional oscillatory angular displacements superimposed on the nominal rotational motions of the object in question. On the one hand, this phenomenon results in severe dynamic overloads leading to dangerous material fatigue of the most heavily affected and responsible elements of these mechanical systems, e.g., shaft segments, joints, and couplings, in too fast wear of gear stage teeth as well as in harmful noise generation and unexpected loss of transmitted energy. On the other hand, during regular operational conditions, torsional vibrations are hardly detectable, and contrary to lateral and axial oscillations of drive systems, they are difficult to measure and monitor. Thus, this problem has been investigated for many years by many authors, which is evidenced not only by numerous research papers but also by classic monographs, see [1, 2].

The well-known, traditional passive methods of attenuation of torsional vibrations described in [1] and applied so far for a long time are not sufficiently effective in the majority of practical applications. However, active and semi-active vibration

control of drive systems of rotating machines, mechanisms, and vehicles creates new possibilities for improvement of their effective operation. Recently observed fast development of active, semi-active, and adaptive control strategies for mechanical systems opens new possibilities for suppressing this detrimental phenomenon. At this point, however, it should be emphasized that torsional vibrations are generally difficult to control, not only from the point of view of generating the appropriate values of control torques but also from the viewpoint of a convenient technique of applying control torques to the quickly rotating elements of the rotating machine drive system. Unfortunately, it is not possible to find so many published research results in this field, apart from a few attempts to actively control the torsional vibrations of shafts using piezoelectric actuators, as seen in [3]. But in such cases, relatively small values of control torque can be generated, so piezoelectric actuators can usually be used in low-power drive systems.

As it follows, from [4–7], for example, an application of rotary dampers with the magneto-rheological fluid (MRF) enables us an effective semi-active suppression of torsional vibrations in several mechanical systems. But in order to generate sufficiently large values of damping torques using such rotary dampers, big masses and geometrical dimensions of these devices are required, respectively.

It should be noted that all the above-mentioned methods of attenuating torsional vibrations of rotating machinery drive systems rely on direct impact on the mechanical system by applying control torques to it, regardless of whether the cause of

*e-mail: tszolc@ippt.pan.pl

Manuscript submitted 2023-07-28, revised 2023-10-17, initially accepted for publication 2023-10-26, published in December 2023.

excitation of these vibrations is a source of the drive itself or power receiver. It turns out, however, that torsional vibrations can be suppressed using the drive source itself, i.e. by means of an electric motor equipped with voltage-frequency inverters and various control systems. Then, the driving electric motor also acts as an actuator controlling the torsional vibrations of the driven mechanical system. For such motors, various control strategies have been developed, which are described in numerous publications, e.g. in [8–19]. In order to prevent machine drive systems against transient torsional overloading, depending on the given electric motor type, several control methods are already quite commonly applied in industrial practice. In [8, 9] by means of the driving electric motor open-loop control attempts were made to avoid the Sommerfeld effects. For asynchronous motors, as in [8] for example, the well-known standard “ $U/f = \text{const}$ ” scalar control method is often applied for many years. However, nowadays more advanced vector closed-loop control approaches have become increasingly common. The most popular are the field orientation control (FOC), direct torque control (DTC), model predictive control (MPC) method, and others, almost all of them with several modifications, as described in [10–13, 15]. Nevertheless, it should be remembered that the vector FOC and DTC control of asynchronous motors is not always able to effectively minimize torsional transient vibrations induced by the motor itself, which was mentioned in [12, 15], and computationally demonstrated in [16]. In connection with the above, even more advanced control algorithms are gradually being developed, such as model predictive control (MPC) described in [15], and direct torque and rotor flux control (DTRFC) used in [17], which can facilitate a possibly effective reduction of amplitudes of torsional vibrations generated not only by electric drive motors but also by energy receivers and other sources. Nevertheless, it is worth emphasizing that the above-mentioned methods and their modifications have been mainly used so far to eliminate torsional transient vibrations caused by sudden changes in the operating conditions of the electromechanical systems and to ensure the most precise parameters of their motion. However, it is very difficult to find in the available literature analogous results of research on the attenuation of steady-state torsional vibrations, especially in resonant conditions.

In the presented paper a suppression of steady-state and transient torsional vibrations of rotating machines driven by asynchronous motors is going to be conducted using an active motor control. The investigations will be performed by means of a structural hybrid mechanical model of the rotating machine drive systems, wherein geometrical dimensions and material constants of the rotor-shaft line segments are thoroughly taken into consideration. These systems are driven by asynchronous motors equipped with control units of a cascade structure consisting of the electromagnetic torque inner loop control and the rotational speed outer loop control. Contrary to the methods of active control of asynchronous motors applied so far, the motors of the tested systems are powered using a power electronic converter with the six insulated-gate bipolar transistor (IGBT) bridge system, which directly controls the electromagnetic moment of the electric motors using the DTC-SVM control strat-

egy. In addition, an alternative, simplified but equally effective approach is originally proposed here, which boils down to an active, closed-loop control of the supply voltage frequency based on monitoring of the current value of the input rotational speed of the driven machine working tool. This approach will be called further “the method of rotational velocity-controlled torque” (RVCT).

2. DESCRIPTION OF THE ROTATING MACHINE DRIVE SYSTEM UNDER TORSIONAL VIBRATIONS

In general, torsional vibrations in machine drive systems are caused by many factors. These may be unbalanced variable components of the resistive torque generated by the driven machine, for example in the case of reciprocating pumps, fluctuations of gear meshing stiffness, gear transmission errors, coupling misalignments, interaction of variable speed transmission units like Cardan joints, and many others. In each of these cases, the induced torsional vibrations are usually characterized by a fundamental harmonic component, the frequency of which may be close to one of the drive systems natural torsional vibration frequencies, threatening the effect of dangerous resonance.

In order to elaborate active control techniques for effective attenuation of torsional vibrations, properly representative drive systems of the rotating machines must be tested. In this paper three typical drive trains will be investigated. In all these drive systems power is transmitted from an asynchronous motor to the driven rotating machine working tool by means of elastic couplings and shaft segments. A common structure of such drive trains is presented in Fig. 1. In this specific case of the drive system, the cause of excitation of torsional vibrations will be the abovementioned fundamental harmonic component of the variable resistive torque of the driven machine applied to its working tool.

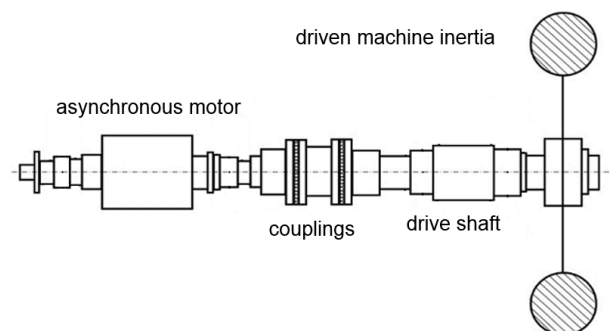


Fig. 1. Scheme of the drive system of the rotating machine driven by an asynchronous motor

To develop a sufficiently reliable control algorithm for the drive system under consideration, the theoretical investigations have to be performed by means of its advanced structural mechanical model. In turn, electrical interactions are going to be investigated here in order to determine in a possibly accurate way the electromagnetic torque produced by the asynchronous motor, which simultaneously drives and controls the operation of the mechanical part. This is particularly essential for a re-

liable and effective active control of torsional vibrations. For this purpose, there is applied a circuit electrical model of the asynchronous motor in the form of voltage ordinary differential equations coupled with motion equations of the abovementioned mechanical model of the drive system. Thus, these two models create an electro-mechanical model of the object under study.

2.1. Assumptions for the mechanical model and its mathematical description

To conduct theoretical studies of the active control of a mechanical system subjected to torsional vibrations, a reliable and computationally efficient simulation model is required. In this work, dynamic tests of the entire drive system will be conducted using a structural hybrid mechanical model, consisting of torsionally deformable one-dimensional continuous finite macro-elements and rigid bodies. Namely, in this hybrid model, the finite macro-elements with continuously distributed visco-inertial-elastic properties represent successive cylindrical segments of a real stepped rotor shaft. In turn, hardly deformable drive system coupling flanges and rotor disks are substituted by rigid bodies attached to the appropriate macro-element extreme cross-sections. Time- or system-dynamic response-dependent external active and passive torques can be distributed continuously along the appropriate finite macro-elements or applied in a concentrated form in given cross-sections of these macro-elements.

Similarly, as in [18] and [19], the torsional motion of cross-sections of each finite macro-element in the hybrid model is governed by the wave-type hyperbolic partial differential equations. Interconnections of the successive macro-elements forming a stepped shaft and their interactions with the rigid bodies are described by equations of compliance conditions, which can be distinguished into two groups. Namely, the first one contains geometrical compatibility conditions for rotational displacements of extreme cross-sections of the adjacent finite macro-elements. The second group, however, includes dynamic conditions of equilibrium for inertial, elastic, and external damping moments as well as for external torques. The solution for natural and forced vibrations is obtained using the analytical-computational approach described and used, e.g. in [18] and [19]. For this purpose, in order to determine system dynamic responses, the differential eigenvalue problem must be solved first, and then an application of the Fourier solution in the form of series in the orthogonal eigenfunctions enables us to obtain the set of uncoupled ordinary differential equations for the modal coordinates $\xi_m(t)$, $m = 1, 2, \dots$,

$$\begin{aligned} \ddot{\xi}_m(t) + (\beta + \tau\omega_m^2)\dot{\xi}_m(t) + \omega_m^2\xi_m(t) \\ = \frac{1}{\gamma_m^2} (\Theta_m^M \cdot T_{el}(t) - \Theta_m^R \cdot M_r(t)), \quad m = 0, 1, 2, \dots \end{aligned} \quad (1)$$

where β denotes the coefficient of external damping assumed here as proportional damping to the modal masses γ_m^2 , τ is the retardation time, ω_m is the successive natural frequencies of the drive system, $T_{el}(t)$ is the external torque generated by the electric motor, $M_r(t)$ denotes the driven machine retarding torque,

and Θ_m^M , Θ_m^R are the modal displacements scaled by proper maxima and corresponding respectively to the electric motor and to the driven machine working tool-locations in the hybrid model. The number of equations (1) corresponds to the number of torsional eigenmodes taken into account in the frequency range of interest to us. In order to obtain a sufficient accuracy of results in this range of frequency, fast convergence of the applied Fourier solution allows one to reduce the appropriate number of modal equations (1) to be solved, usually to only a few or a dozen. For comparison, in the analogous case of applying classical one-dimensional modelling by means of the finite element method, in order to avoid solving dozens or even hundreds of equations in generalized (natural) coordinates, well-known, often numerical error-prone, degree of freedom reduction methods must be used.

2.2. Modelling of the asynchronous motor

Torsional vibrations of the drive system usually cause significant rotational speed fluctuations of the rotor of the driving electric motor. Such fluctuations of the angular velocity superimposed on the average rotational speed of the rotor cause a more or less strong disturbance of the electromagnetic flux, and thus additional oscillations of electric currents in the motor windings. Then, the generated electromagnetic motor torque is also characterized by additional time-varying components that induce torsional vibrations of the drive system. Accordingly, the mechanical vibrations of the drive system are coupled with the oscillations of the electric currents in the motor windings. Such a coupling is often complex in nature, and therefore computationally troublesome. For this reason, so far, most authors have simplified the matter by treating torsional vibrations of drive systems and electric current oscillations in motor windings as mutually uncoupled. Then, mechanical engineers usually describe the electromagnetic torques generated by electric motors in the form of ‘a priori’ adopted functions of time or slip of the motor rotor relative to the motor stator, as, e.g. in [2]. Such functions were most often determined using results of experimental measurements conducted for many scenarios of the dynamic behavior of a given electric motor.

However, electrical engineers, on the one hand, very accurately model time courses of the generated electromagnetic torques based on advanced theories of operation of a given type of electric motor, but on the other hand, they almost always reduce the mechanical drive system to one or rarely to several rotating rigid bodies mutually connected by linear springs, see [9, 12–14]. In many cases, such simplifications give insufficiently accurate results, both for the mechanical and electrical parts of the tested objects.

In order to develop an appropriate control algorithm for a given torsionally vibrating drive system, the external electromagnetic excitation generated by the driving motor should be described as precisely as possible. Therefore, the electromechanical coupling between the electric motor and the drive train must be also taken into account as closely as possible. Thus, in addition to the realistic, structural hybrid model of the torsionally vibrating mechanical object described above, it is necessary to introduce a possibly reliable mathematical model of the

electric motor. In the case of a symmetrical three-phase asynchronous motor considered here, oscillations of electric currents in its windings are usually described by six voltage equations in the so-called coordinate system of natural axes A-B-C, as presented in [20, 21], for example. By the use of Clarke's transformation into the two mutually perpendicular electrical axes $\alpha - \beta$ a number of these equations can be reduced to four:

$$\mathbf{U}_s = \mathbf{R}_s \mathbf{i}_s + \frac{d\boldsymbol{\Psi}_s}{dt}, \quad \mathbf{0} = \mathbf{R}_r \mathbf{i}_r + \frac{d\boldsymbol{\Psi}_r}{dt}, \quad (2)$$

where:

$$\begin{aligned} \mathbf{U}_s &= \begin{bmatrix} U_\alpha^s(t) \\ U_\beta^s(t) \end{bmatrix}, \quad \mathbf{R}_s = \begin{bmatrix} R_1 & 0 \\ 0 & R_1 \end{bmatrix}, \\ \mathbf{L}_s &= \begin{bmatrix} L_1 + \frac{1}{2}M & 0 \\ 0 & L_1 + \frac{1}{2}M \end{bmatrix}, \\ \mathbf{L}_m(p\theta) &= \frac{3}{2}M \begin{bmatrix} \cos(p\theta) & -\sin(p\theta) \\ \sin(p\theta) & \cos(p\theta) \end{bmatrix}, \quad \mathbf{R}_r = \begin{bmatrix} R'_2 & 0 \\ 0 & R'_2 \end{bmatrix}, \\ \mathbf{L}_r &= \begin{bmatrix} L'_2 + \frac{1}{2}M & 0 \\ 0 & L'_2 + \frac{1}{2}M \end{bmatrix}, \\ \boldsymbol{\Psi}_s &= \mathbf{L}_s \cdot \mathbf{i}_s + \mathbf{L}_m(p\theta) \cdot \mathbf{i}_r, \quad \boldsymbol{\Psi}_r = \mathbf{L}_m^T(p\theta) \cdot \mathbf{i}_s + \mathbf{L}_r \cdot \mathbf{i}_r, \\ \mathbf{i}_s &= [i_\alpha^s(t), i_\beta^s(t)]^T, \quad \mathbf{i}_r = [i_\alpha^r(t), i_\beta^r(t)]^T, \end{aligned}$$

$U_\alpha^s(t)$ and $U_\beta^s(t)$ denote the supply voltage components, R_1, R'_2 is the stator coil resistance and the equivalent rotor coil resistance, respectively, M denotes the relative rotor-to-stator coil inductance, L_1, L'_2 is the stator coil inductance and the equivalent rotor coil inductance, respectively, p is the number of pairs of the motor magnetic poles, $\theta = \theta(t)$ denotes the rotation angle between the rotor and the stator, and $i_\gamma^q, \gamma = \alpha, \beta$, are the electric currents in the stator for $q = s$ and in the rotor for $q = r$, reduced to the electric field equivalent axes α and β , see [20, 21]. Then, the electromagnetic torque generated by such a motor can be expressed as a function of the stator flux linkage components Ψ_α^s and Ψ_β^s :

$$T_{el} = p \left[\Psi_\alpha^s \cdot i_\beta^s - \Psi_\beta^s \cdot i_\alpha^s \right], \quad (3)$$

where the amplitude Ψ_s of vector $\boldsymbol{\Psi}_s = [\Psi_\alpha^s, \Psi_\beta^s]^T$ and its phase angle δ_ψ are respectively equal to:

$$\Psi_s = \sqrt{(\Psi_\alpha^s)^2 + (\Psi_\beta^s)^2}, \quad \delta_\psi = \arctan \left(\frac{\Psi_\beta^s}{\Psi_\alpha^s} \right). \quad (4)$$

The form of expression (3) for the motor torque is useful for modelling the control algorithm as well as for the determination of the current torque values generated by a real motor, since the stator electric currents are relatively easy to measure, and the stator flux is convenient to estimate. From the modal equations (1), the system of voltage equations (2), as well as for-

mula (3), it follows that the coupling between the electrical and mechanical system is non-linear, which leads to a complicated analytical description leading consequently to a rather difficult computer implementation. Thus, the effect of this electromechanical coupling is realized here by the use of a direct integration method coupled step-by-step with the cubic numerical extrapolation technique, which, with relatively small integration steps applied to equations (1) and (2), gives highly effective, stable and reliable computer simulation results.

3. MODELLING OF THE ASYNCHRONOUS MOTOR CONTROL SYSTEM

An operation algorithm of the driving motor control system is based on a mathematical model describing the actions of the speed regulator as well as electromagnetic torque and stator magnetic flux linkage. Here, three quantities will be controlled when using the DTC-SVM method for an asynchronous motor. These are the angular velocity registered at the motor rotor, the electromagnetic motor output torque, and the stator flux linkage. For all of them, the PI control strategy is applied in order to minimize their control deviations with respect to the expected required values.

The scheme according to [12] of the standard DTC-SVM control algorithm applied here for the asynchronous motor driving the rotating system under study is presented in Fig. 2a. In this figure Ψ_{ref} denotes the stator flux reference controlling signal, T_{ec} is the electromagnetic torque controlling signal, $\hat{\Psi}_s$ denotes the estimated stator flux amplitude, \hat{T}_e is the estimated electromagnetic torque, $\hat{\delta}_\psi$ denotes the stator flux estimated angle, \mathbf{U}_s is the determined stator voltage vector, \mathbf{U}_{sc} denotes the stator voltage controlling vector, U_{scx} is the flux component of the voltage controlling vector, U_{scy} denotes the torque component of the voltage controlling vector, \mathbf{I}_s is the measured electric current vector, $S_{A,B,C}$ denote the transistor gate signals, $I_{A,B,C}$ are the measured currents in stator phases A, B, C, and U_{DC} denotes the measured inverter DC link voltage. The outer velocity control loop is depicted in Fig. 2b. In addition to the above-mentioned symbols in this figure, $\tilde{\omega}_{ref}$ denotes the demanded reference velocity and ω_M is the measured mechanical velocity of the motor shaft.

In the system under consideration, the momentary supply voltage value must be properly determined to achieve the expected values of the motor output torque and stator flux linkage. As it follows from [12] and [15], in the stator coordinate frame x - y rotating together with the stator flux vector $\boldsymbol{\Psi}_s$ the supply voltage component U_{SX} is proportional to the change in time of the stator flux amplitude Ψ_s , and the supply voltage component U_{SY} is proportional to the motor output torque T_{el} , what can be expressed by the following relationships:

$$U_{SX} \Rightarrow \frac{d\Psi_s}{dt} \quad \text{and} \quad T_{el} \Rightarrow \frac{3p}{2R_1} \Psi_s U_{SY}. \quad (5)$$

Consequently, by means of proper values of the supply voltage in time $U_{SX}(t)$ and $U_{SY}(t)$ the required changes of the stator flux amplitude $\Delta\Psi_s$ and the motor torque T_{el} can be achieved

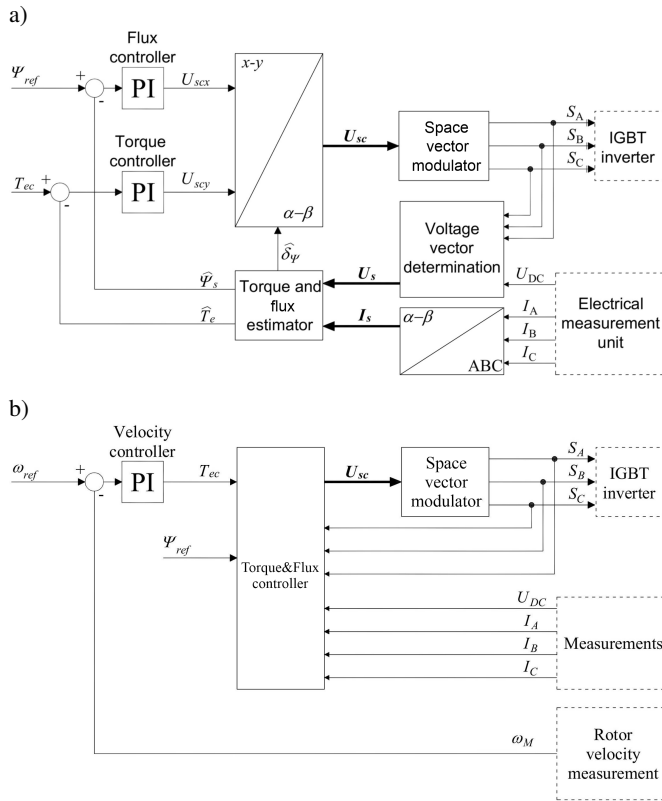


Fig. 2. Scheme of the asynchronous motor control using the DTC-SVM method, [12]: a) structure of torque and stator flux estimators with adjacent controllers and the modulator governing IGBT inverter; b) velocity control loop depicting the emplacement of the controller part

according to (5). Further going, the required changes of the stator flux amplitude $\Delta\Psi_S$ and the motor torque T_{el} are being obtained using the PI control in the following way:

$$T_{el} = k_{PT} \cdot T_{el}^{err} + k_{IT} \cdot \int_0^t T_{el}^{err} d\tau \quad \text{and} \quad (6)$$

$$\Delta\Psi_S = k_{P\Psi} \cdot \Psi_S^{err} + k_{I\Psi} \cdot \int_0^t \Psi_S^{err} d\tau,$$

where T_{el}^{err} and Ψ_S^{err} denote the control deviations of the motor output moment and stator flux amplitude, respectively, and k_{PT} , k_{IT} , $k_{P\Psi}$, $k_{I\Psi}$ are their proportional and integral gains. The voltage instantaneous values $U_{SX}(t)$ and $U_{SY}(t)$ obtained by means of formulae (5) and (6) must be transformed next into the non-rotating coordinate frame α - β and then used as the supply voltage components $U_{\alpha}^S(t)$ and $U_{\beta}^S(t)$ standing in (2). In order to keep the resultant supply voltage value in the admissible rated motor voltage regime, the anti-wind-up routine for integral control of the motor output torque and flux linkage is applied when $U_{SX}(t)$ and $U_{SY}(t)$ voltage components are determined.

$$\begin{aligned} U_{\alpha}^S(t) &= U_{SX}(t) \cos(\delta\psi) - U_{SY}(t) \sin(\delta\psi), \\ U_{\beta}^S(t) &= U_{SX}(t) \sin(\delta\psi) + U_{SY}(t) \cos(\delta\psi). \end{aligned} \quad (7)$$

It is assumed that the hardware implementation of the vector control system presented above uses a classic three-phase bridge system with IGBT transistors and energy storage in the form of a capacitor. Then, when the vector control SVM is applied, the switching frequency f_s of the voltage supplied to the motor, equal to 16 kHz in the case under study, is high enough to ensure a sufficiently smooth course of currents in the motor windings. Therefore, it is legitimate to approximate the model of a transistor converter by a first-order inertial term with a time constant equal to $T_s = 1/f_s$. Due to the above, it is reasonable to describe the supply voltage waveforms by means of harmonic functions when conducting computer simulations.

Alternatively, the standard DTC-SVM method described above will be compared with a simplified, but effective and robust approach based on the motor voltage supply frequency dependent on the momentary value of rotational velocity of the driven machine working tool registered by a speed controller, where the supply voltage is assumed constant in time. Namely, under steady-state operating conditions the actual value of the supply voltage is related to the constant rotational speed of the motor rotor so that for the rated, nominal speed, this voltage is equal to the maximum value available in the electric network. Here, this alternative approach is physically realized by means of the mechanical part of the drive train, speed sensor, and speed controller only. A scheme of this system is illustrated in Fig. 3.

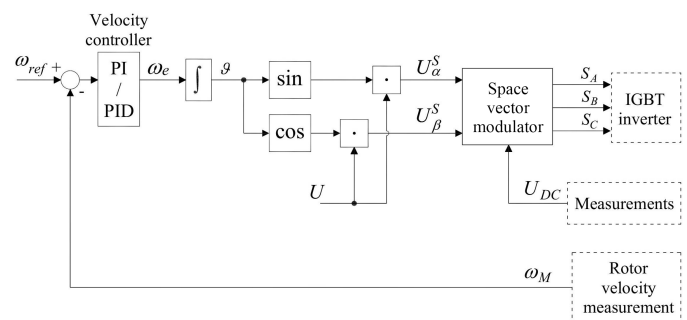


Fig. 3. Scheme of the asynchronous motor control using the originally proposed RVCT method

Using the standard PI or PID control, the supply voltage frequency is ensured according to the current rotational speed value of the driven machine working tool in relation to the specified reference value ω_M . Thus, it will be called further “the method of rotational velocity-controlled torque” (RVCT). In this case, instead of projecting the supply voltage components $U_{SX}(t)$ and $U_{SY}(t)$ on the non-rotating co-ordinate axes α and β by means of relationships (7), the proper constant value U of the supply voltage vector is transformed into the non-rotating coordinate frame α - β :

$$U_S = \begin{bmatrix} U_{\alpha}^S(t) \\ U_{\beta}^S(t) \end{bmatrix} = \begin{bmatrix} \sqrt{\frac{3}{2}} U \cos(\vartheta(t)) \\ \sqrt{\frac{3}{2}} U \sin(\vartheta(t)) \end{bmatrix}, \quad (8)$$

where: $\vartheta(t) = \int_0^t \omega_e(\tau) d\tau$, and $\omega_e(t)$ denotes the supply circular frequency determined using the PI or PID closed-loop control of the driven machine rotational velocity.

For the assumed sinusoidal external excitation $M_r(t) = R \cdot \sin(\omega t)$ generated by the driven machine working tool at the current angular velocity $\Omega(t) = \Omega_n + \Theta(t)$ consisting of the average Ω_n and vibratory $\Theta(t)$ component, $\Theta(t)$ is also expected harmonic with the same frequency ω : $\Theta(t) = G \cdot \sin(\omega t) + H \cdot \cos(\omega t)$, where $|G|, |H| \ll \Omega_n$. Then, as demonstrated in [18], the fluctuating component of the motor torque is induced, which can be sought in the following harmonic form:

$$T_v(t) = A(\omega) \sin(\omega t) + B(\omega) \cos(\omega t), \quad (9)$$

where:

$$T_v(\omega) = \sqrt{A^2(\omega) + B^2(\omega)} \text{ and } \chi(\omega) = \arctan(B(\omega)/A(\omega)).$$

According to [18], the excitation frequency-dependent amplitudes $A(\omega)$ and $B(\omega)$ can be determined when using the harmonic balance method for the asynchronous motor voltage equations (2) subjected to Park's transformation. Then, the following system of 16×16 linear algebraic equations describing electromechanical coupling is obtained:

$$\mathbf{C}(\Omega_n, \omega_e, \omega, \omega_m, \gamma_m^2, \beta, \tau) \cdot \mathbf{D}(A(\omega), B(\omega)) = \mathbf{F}(\omega_m, \gamma_m^2, \beta, \tau, \omega, R). \quad (10)$$

Here, matrix \mathbf{C} as well as the input vector \mathbf{F} are functions of the mechanical system dynamic parameters, and the sine- and cosine- amplitudes $A(\omega)$ and $B(\omega)$ of the electromagnetic torque fluctuating component $T_v(\omega)$ can be determined by solving equation (10) with respect of the unknown vector \mathbf{D} for the given retarding torque amplitude R in a required range of the external excitation frequencies ω . Then, using (9) and by means of the proper motor control method DTC-SVM or RVCT, the electromagnetic torque amplitude $T_v(\omega)$ and the phase angle $\chi(\omega)$ can be properly adjusted to eliminate excitations of successive torsional eigenmodes in the modal equations (1):

$$T_v(t) \approx \frac{\Theta_m^R}{\Theta_m^M} R \sin(\omega t), \quad m = 1, 2, \dots \quad (11)$$

It is worth noting that in order to achieve this target for the first, fundamental torsional eigenmode, i.e. for $m=1$, the electromagnetic and retarding torque must mutually oscillate in anti-phase with properly tuned up amplitudes.

It is worth remembering that in the literature, e.g. in [22], some attempts were made in order to investigate qualitatively the abovementioned non-linear coupling between the driven mechanical system and the driving electric motor. To follow this idea here, it would be necessary, similarly as in [22], to express the electromagnetic motor torque as a function of squares and cubes of the current rotation angle $\theta(t)$. Simultaneously, the rotational motion of the mechanical system under study should be reduced to an analogous motion of a torsional oscillator of one degree of freedom described by $\theta(t)$. Then, by means of

such a single degree of freedom of a nonlinear electromechanical system, a standard qualitative and stability analysis could be performed. However, since the main target of this paper is an elimination of external torsional excitations according to formula (11) by means of the closed-loop active control using the driving asynchronous motor, such additional qualitative study of the electromechanical system nonlinearity seems to be unnecessary.

4. COMPUTATIONAL EXAMPLES

Numerical calculations have been performed for three electromechanical drive systems of the common structure presented in Fig. 1, but with different powers, total mass moments of inertia, and nominal rotational speeds. These are: "1" – the laboratory rotor drive system, "2" – the drive of the high-speed beater mill used for grinding natural resources, and "3" – the drive of the heavy industrial fan. Fundamental parameters of their electronically controlled asynchronous motors are collected in Table 1. Static characteristics of the examined motors naturally differ within their rotational speed ranges in starting and maximal torque values. However, the particular qualitative differences of these characteristics are the average angles of inclination of their parts corresponding to the range of stable operation. Such mutual differences have been illustrated in Fig. 4a by means of three variants of the exemplary static characteristics of a given asynchronous motor. It is worth noting that these characteristics were obtained by means of two methods each, i.e. using the Kloss formula commonly found in numerous handbooks of electric engineering, and by means of the analytical solution of equations (2) transformed into the form of Park's equations, as described in detail in [18]. In this figure the plot marked in green corresponds to the motor "soft" static characteristics, the plot marked in blue to the "medium" characteristics, and the plot marked in red to the "stiff" one, respectively. In this sense, the asynchronous motor in drive system "1" has "soft" static characteristics, in drive system "2" has "medium" characteristics, and in the case of "3" – "stiff" characteristics. The actual static characteristics of these three motors can be easily determined using the numerical parameters contained in Table 1.

In turn, the rotating part of a driven machine can be relatively more "massive" or "lighter" than the rotor of its driving motor, which results in different fundamental torsional first eigenforms of the drive system of that object. Such exemplary first eigenforms obtained for the laboratory rotor drive system mentioned above are depicted in Fig. 4b. In the case of "heavy motor" an absolute eigenfunction value Θ_1^M of the driving end (D-E) is smaller than that of the driven end (N-E) Θ_1^R .

However, when the inertia of the driven machine is greater than that of the motor rotor, the absolute eigenfunction value Θ_1^M of the driving end (D-E) is bigger, respectively. For similar mass moments of inertia of the driven machine and motor rotor, eigenfunction absolute modal displacement values of the driving (D-E) Θ_1^M and driven end (N-E) Θ_1^R are comparable or even equal to each other, but with mutually opposite signs, as shown in Fig. 4b.

Suppression of rotating machine shaft-line torsional vibrations by a driving asynchronous motor using two advanced control methods

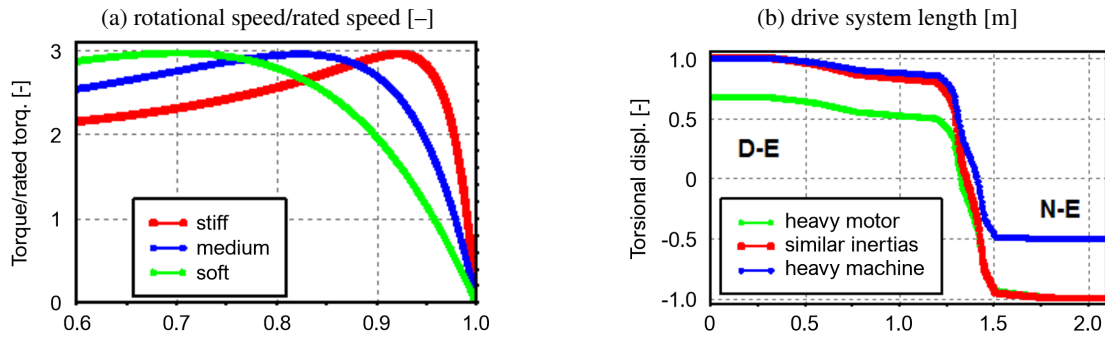


Fig. 4. Static characteristics of the asynchronous motors (a) and variants of the fundamental torsional eigenmode of the drive system

Table 1

Fundamental technical parameters of the asynchronous motors under study

Motor number	“1 – soft”	“2 – medium”	“3 – stiff”
Maximal power [kW]	3.8	200	3200
Supply voltage [V]	390 (Y)	500 (Δ)	6000 (Y)
Supply frequency [Hz]	60	50	50
Nominal rotational speed [rpm]	1680	2979	747
Number of pole pairs [-]	2	1	4
Nominal rated torque [Nm]	21.5	641	40907.3
Stator resistance [Ohm]	1.52	0.0302	0.0757
Rotor eq. resistance [Ohm]	1.37	0.0192	0.07554
Stator reactance [Ohm]	2.1074	0.1978	1.2514
Rotor eq. reactance [Ohm]	2.277	0.2835	1.04885
Mutual reactance [Ohm]	54.287	17.7	13.0951

Table 2

Fundamental dynamic parameters of the laboratory rotor drive system

Drive system variant	“heavy machine”	“similar inertias”	“heavy motor”
Motor rotor mass moment of inertia [kgm ²]	0.0036		
Total mass moment of inertia of the drive system [kgm ²]	0.2676	0.1786	0.1476
Modal mass γ_1^2 of the 1st torsional eigenmode [kgm ²]	0.1120	0.1369	0.0686
The 1st torsional eigenfrequency $\omega_1/2\pi$ [Hz]	48.470	57.258	66.080
Retardation time τ of the structural damping [s]	0.0000234		

Table 3

Fundamental dynamic parameters of the high-speed beater mill drive system

Drive system variant	“heavy machine”	“similar inertias”	“heavy motor”
Motor rotor mass moment of inertia [kgm ²]	1.74		
Total mass moment of inertia of the drive system [kgm ²]	5.2763	3.5263	2.9363
Modal mass γ_1^2 of the 1st torsional eigenmode [kgm ²]	2.6309	3.4919	1.9343
The 1st torsional eigenfrequency $\omega_1/2\pi$ [Hz]	36.509	42.179	47.228
Retardation time τ of the structural damping [s]	0.0000234		

Fundamental dynamic parameters of the three electro-mechanical drive systems under study, which result in eigen-vibration properties illustrated in Fig. 4b, are contained in Tables 2, 3, and 4, respectively for the laboratory rotor drive system “1,” drive of the high-speed beater mill “2” and drive of the heavy industrial fan “3”. The common value of the retardation time τ of the structural damping in these three drive systems follows from the typical, relatively small loss-factor values for steel. These properties significantly affect the sensitivity to external excitations and the ability to control the vibrations of the first torsional eigenforms of the electromechanical systems under study. This can be expressed in the form of amplitudes $T_v(\omega)$ of the variable component of the electromagnetic torque generated by the asynchronous motor. For the three asynchronous motors with “soft,” “medium” and “stiff” static characteristics and the three abovementioned variants of the motor rotor to driven machine inertia ratios, Fig. 5 depicts such amplitude characteristics obtained by solving equation (10) for motor steady-state, nominal operating conditions, as related to the amplitude of the external excitation produced by the driven object. They are a measure of asynchronous motor

torque sensitivity to fluctuations induced by torsional vibrations of the mechanical system. All these plots are characterized by maximal peak values corresponding respectively to the first torsional natural frequency of the rotating machine drive system. This means, that the asynchronous motors are the most sensitive to generating fluctuating components of their electromagnetic torque in resonant operational conditions. Based on the

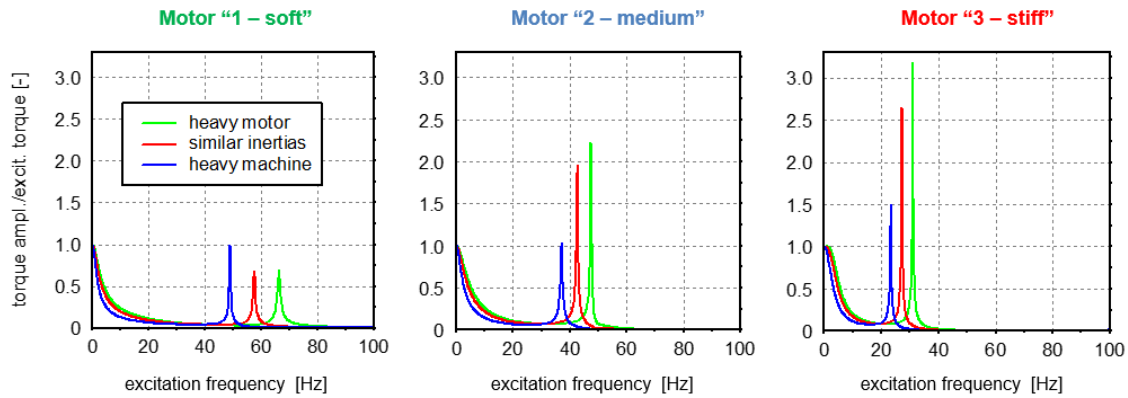


Fig. 5. The characteristics of the electromagnetic motor torque amplitudes related to the amplitude of excitation caused by the driven machine

graphs shown in Fig. 5, it can be concluded that the greater the stiffness of the motor static characteristics, the greater the value of the maximum amplitude of the generated torque $T_v(\omega)$. It should be noted that all plots presented in Fig. 5 were obtained in the case of an uncontrolled motor operation. Due to an appropriate control of the asynchronous motor, the variable component of the electromagnetic torque $T_v(\omega)$ can be properly tuned in terms of its amplitude and phase, so that condition (11) is satisfied, which facilitates an effective minimization of a given eigenform, e.g. the first one of torsional vibrations of the drive system under consideration.

Table 4

Fundamental dynamic parameters of the heavy industrial fan drive system

Drive system variant	“heavy machine”	“similar inertias”	“heavy motor”
Motor rotor mass moment of inertia [kgm ²]	445.3		
Total mass moment of inertia of the drive system [kgm ²]	1807.6	1202.6	996.63
Modal mass γ_1^2 of the 1st torsional eigenmode [kgm ²]	827.16	1036.7	554.26
The 1st torsional eigenfrequency $\omega_1/2\pi$ [Hz]	22.919	26.965	30.836
Retardation time τ of the structural damping [s]	0.0000234		

By means of numerical simulations, the degree of achieving this goal using DTC-SVM and RVCT control will be demonstrated for the three electromechanical drive systems under consideration and for all three variants of the ratio of the mass moment of inertia of the motor rotor to the mass moment of inertia of the driven machine. For this purpose each drive system will be subjected to the following motion scenario: First, it will be started up from its standstill to nominal operational conditions by means of the classic open-loop scalar motor control $U/f = \text{const.}$ Next, to the rated load of the driven machine,

there will be added an oscillating harmonic component with an amplitude equal to 15% of the nominal motor torque and a resonant frequency corresponding to the drive system fundamental, first torsional eigenform. Then, after successive few seconds of an operation under resonant conditions, the vector DTC-SVM and RVCT control will be turned on to suppress the resonance until the end of its duration, and to continue to ensure the precision of parameters of further motion of the drive system. For the three electromechanical systems under study, using various methods several values of control gains were tested in order to select the most optimal ones. In the case of the DTC-SVM method, the highest effectiveness was assured for the stator flux linkage control by means of the symmetrical optimum method, and for the torque control using the root locus approach. In turn, for the RVCT control, the well-known Ziegler-Nichols method turned out to be the most convenient. All controller gains mentioned above ensure the overall stability of the entire electromechanical system.

In Figs. 6a-c there are demonstrated abilities of the control methods applied here to attenuate severe torsional vibrations in these three drive systems under consideration, i.e. in the laboratory drive system driven by “motor “1 – soft,” drive system of the high-speed beater mill driven by motor “2 – medium” and the drive system of a heavy industrial fan driven by motor “3 – stiff,” respectively, all in the case of the variant of similar mass moments of inertia of the motor rotor and the driven machine. In all these figures, time histories of the electromagnetic motor torque (blue lines), driven machine retarding torque (black lines), and dynamic torque transmitted by the coupling (red lines) during the above-described motion scenario are plotted. On the left-hand sides of these figures, there are time windows corresponding to the steady-state motion phase, when the scalar motor control $U/f = \text{const.}$ is applied. From the courses of the electromagnetic motor torque $T_{el}(t)$ and the driven machine retarding torque $M_r(t)$ in these time windows one can easily observe to what extent condition (11) is not satisfied, both in terms of tuning the torque amplitude T_v and the phase angle χ . In turn, in the middle parts of Figs. 6a-c, time windows corresponding to motion intervals of the DTC-SVM (above) and RVCT (below) control are depicted. Here, the respective plots demonstrate, how more or less precisely both motor control

Suppression of rotating machine shaft-line torsional vibrations by a driving asynchronous motor using two advanced control methods

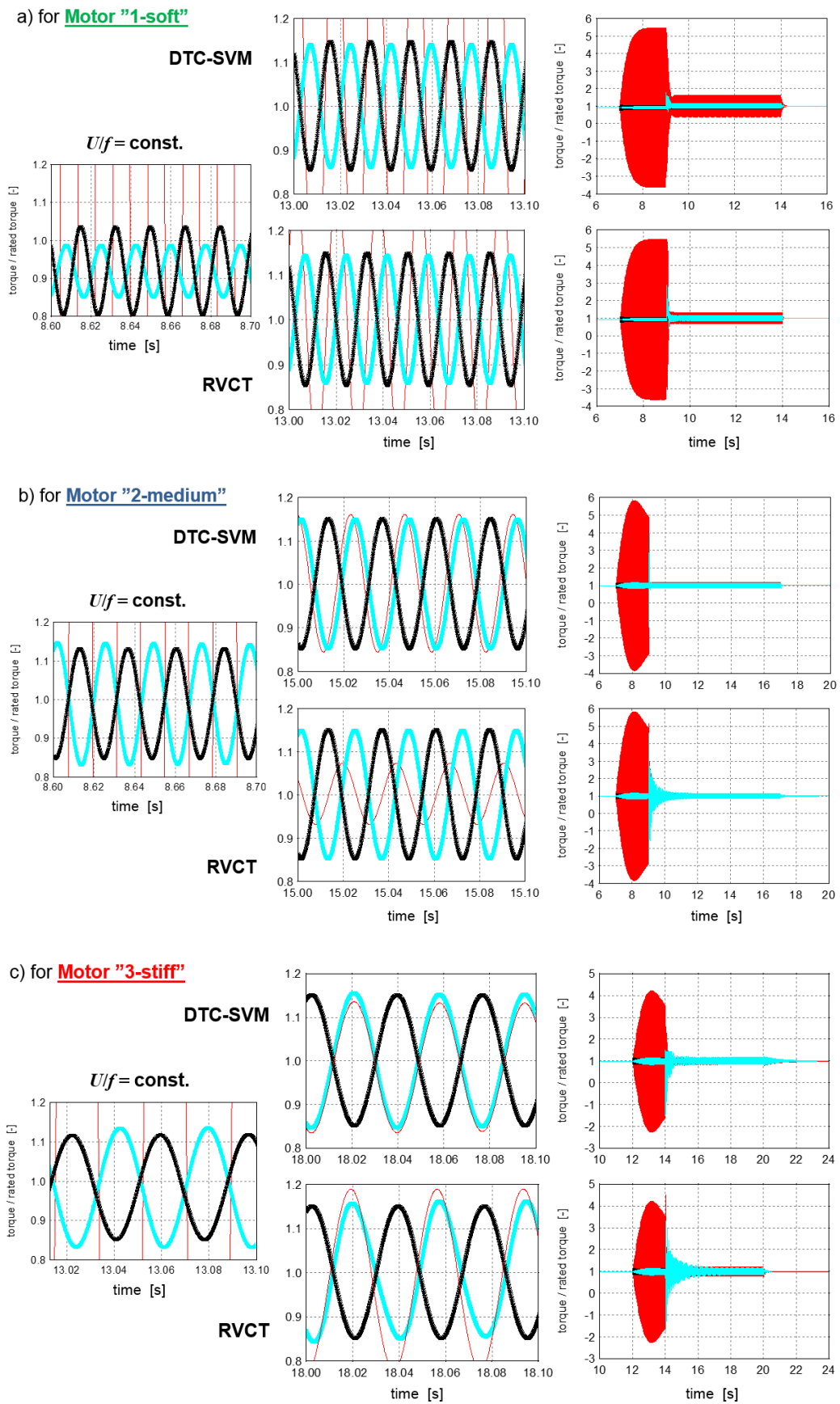


Fig. 6. Dynamic torques controlled by the asynchronous motors driving: the laboratory rotor with motor "1 – soft" (a), the beater mill with motor "2 – medium" (b) and the industrial fan with motor "3 – stiff" (c)

methods being tested mutually tune fluctuations of $T_{el}(t)$ and $M_r(t)$ in order to achieve condition (11) satisfied. Namely, in all studied cases of the drive systems, when applying both control methods, the motor torque $T_{el}(t)$ and the machine retarding torque $M_r(t)$ mutually oscillate in anti-phase with similar amplitude values. This results in the very significant suppression of torsional vibration resonances induced by the driven machine retarding torque $M_r(t)$, which follows from the plots of time histories of the entire motion scenarios placed on the right-hand sides of Figs. 6a-c.

When comparing the effectiveness of the asynchronous motor control routines being tested, the dynamic amplification factors during resonance are regarded here as a fundamental criterion. Such a factor is defined as the ratio of the actual vibration amplitude to the amplitude of the external excitation, i.e. in the case of the conducted tests – the aforementioned 15% of the value of the nominal torque transmitted by the drive system. Table 5 presents values of the dynamic amplification factors in conditions of torsional vibration resonance with the first eigenmodes obtained using DTC-SVM and RVCT control methods for the three electro-mechanical drive systems under consideration and for all three variants of the ratio of the mass moment of inertia of the motor rotor to the mass moment of inertia of the driven machine. In addition, this table also includes for comparison the amplitude amplification factors obtained in the initial phases of resonances, when the tested drive systems were subjected to the open-loop control $U/f = \text{const}$. The numerical values of these factors, which are many times higher than the analogous values obtained using both closed-loop active control methods, result from a relatively high sensitivity to torsional vibrations of drive systems made mainly of steel with typically low loss-factor within the range of 0.00337–0.00972 associated here with the retardation time τ given in Tables 2–4. Analyzing the values of all dynamic amplification factors in Table 5, it should be stated that both closed-loop active control approaches are generally highly effective as compared to the open-loop control $U/f = \text{const}$. Moreover, one can observe that using the simpler RVCT method better results are obtained in the cases of drive systems driven by motor “1 – soft” and motor “2 – medium”. Here, due to the control by means of this approach, the dynamic torque vibration amplitudes are minimized

to become comparable or even smaller, i.e. with amplification factors < 1 , than the fluctuation amplitudes of the driven machine retarding torque $M_r(t)$, as demonstrated in Figs. 6a, b, and Table 5. However, in the case of the industrial fan drive system driven by motor “3 – stiff” a better attenuation was achieved when the DTC-SVM control method was used, which is shown in Fig. 6c.

It is worth noting that in the cases of all tested drive systems, the DTC-SVM control method works quicker than the RVCT approach, causing the resonant torsional vibrations to dissipate faster over time. In addition, the transient response peaks induced when the active motor control is turned on are smaller when using the DTC-SVM method. This fact is confirmed by the corresponding dynamic responses of all three tested drive systems in the form of time histories of rotational speeds registered at their motor ends (blue lines) and driven machine ends (black lines), as shown in Fig. 7. Moreover, the graphs presented in this figure show that both proposed methods of asynchronous motor control cause a fast and precise correction of the rotational speed of the drive system to the desired value (per unit) in relation to the speed obtained by means of the scalar open-loop control $U/f = \text{const}$.

At the end of the testing of both methods of asynchronous motor control, it is worth comparing their impact on power consumption. In Fig. 8, in the same way, as it was done for the rotational speeds, for all three types of motors and the variant of the drive system with “similar inertias,” there are presented time histories of the consumed electric power and the mechanical power performed during the assumed above-mentioned motion scenarios of the electromechanical systems under consideration. Here, according to [23], the electric power was determined in the form of instantaneous power expressed as a sum of products of instantaneous voltages and currents in both electric coordinates α and β . In turn, the mechanical power was calculated as a product of instantaneous values of the motor output torque and shaft angular velocity. Similarly to the case of dynamic torques and rotational speeds discussed above, the RVCT method is characterized by the induction of much more severe transient states in the moments of switching on the active control and slower operation in the form of longer decay of these states over time. Based on the time histories shown in Fig. 8, it can be stated that when both control methods are used, the average values of the electric power consumed are very similar. However, when applying the DTC-SVT method to control motor “1 – soft” and motor “3 – stiff,” the time histories of instantaneous electric powers are characterized by much greater oscillations around their average values than in the case of using the RVCT method, even in the phase of only constant load transmitted by the drive system. This fact is due to significant, i.e. with an amplitude of ca. 30% of the maximal admissible limit, and not presented here in a graphical form, high-frequency oscillations of the instantaneous value of the control voltage using the DTC-SVM method, in contrast to the RVCT approach, in the case of which this voltage is constant over time, as mentioned in the previous section. This effect was not observed in the case of control of motor “2 – medium”.

Table 5

Dynamic amplification factors during resonances

$U/f = \text{const}$	DTC-SVT	“heavy machine”		“similar inertias”		“heavy motor”	
	RVCT						
Motor “1 – soft”	23.3	1.633	29.8	4.067	31.3	7.313	
		1.995		2.019		3.587	
Motor “2 – medium”	15.6	0.553	32.0	1.087	43.3	1.433	
		0.140		0.503		0.301	
Motor “3 – stiff”	10.5	0.833	21.6	1.003	28.7	1.107	
		0.897		1.367		2.167	

Suppression of rotating machine shaft-line torsional vibrations by a driving asynchronous motor using two advanced control methods

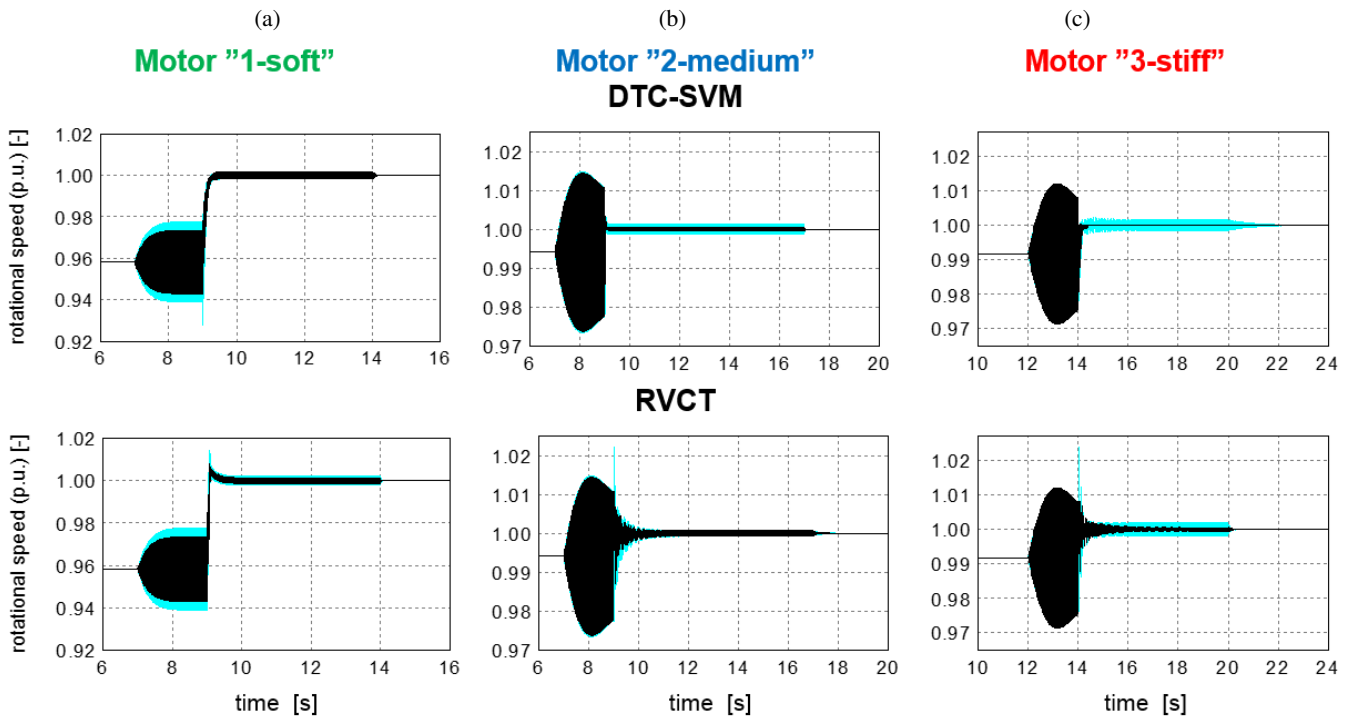


Fig. 7. Rotational speeds controlled by the asynchronous motors driving: the laboratory rotor with motor “1 – soft” (a), the beater mill with motor “2 – medium” (b) and the industrial fan with motor “3 – stiff” (c)

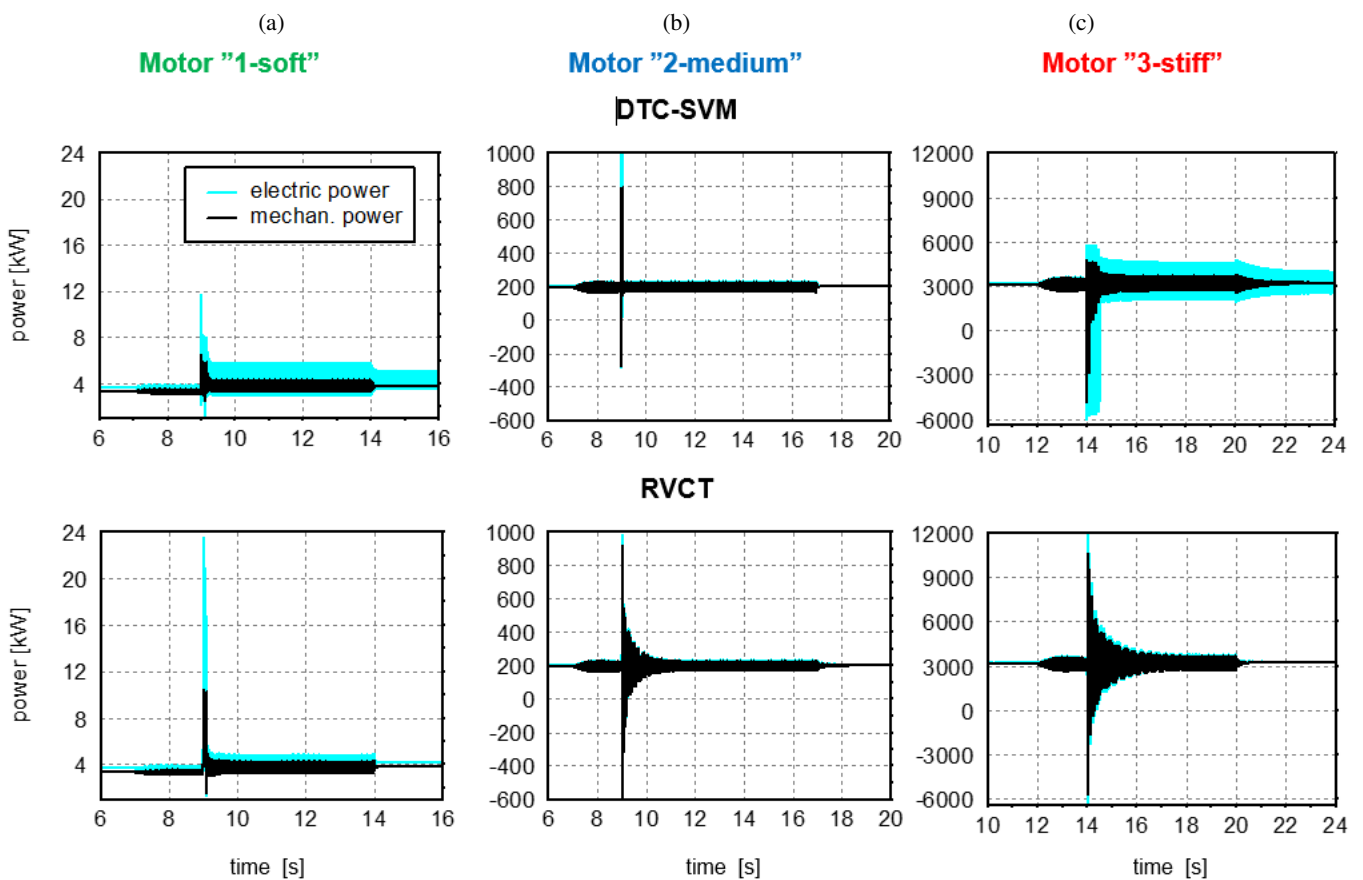


Fig. 8. Electric and mechanical powers consumed during the control of the asynchronous motors driving: the laboratory rotor with motor “1 – soft” (a), the beater mill with motor “2 – medium” (b), and the industrial fan with motor “3 – stiff” (c)

5. REMARKS ON THE RELIABILITY OF THE OBTAINED THEORETICAL RESULTS

When conducting simulations, it is necessary to take into account delays and phase shifts introduced by the measurement, computing, and executive systems that are elements of real power electronic systems. Usually, in variable speed drive systems the useful current and voltage frequency range is often nominally within 0 to 50–60 Hz, in rare cases up to 400 Hz, and in order to filter current/voltage transient states occurring when commutating diodes and transistors, a filter with a specified cut-off frequency is applied. In the presented cases of numerical simulations, the first-order filter with a cut-off frequency of 885 Hz is used. Moreover, it is assumed that the DC-link supply voltage measurement system is also equipped with a first-order filter with the same parameters. In such situations for an inverter output frequency of 60 Hz the phase delay is hence less than 2° .

In the drive systems under study measurements of phase voltages of the inverter are usually not performed and proper estimations are applied instead. These estimations are based on the value of the momentary PWM signal duty cycle and the instantaneous voltage value in the DC-link. Filters with a higher cut-off frequency, e.g. within 100–400 kHz, are connected in a cascade to the above-mentioned filters. Such a high cut-off frequency has practically no effect on delays in the useful measurement range, but it facilitates suppressing the radio interferences from the electronic system of the inverter and eliminates measurement noise effects. Here, all the above-mentioned input filters were assumed to be implemented and modeled in the simulation cases under consideration. In turn, no type of filtration was used during the rotational speed and position measurements, as its accuracy highly influences the quality of the control. In reality, encoders of 10 000 pulses per revolution are successfully applied.

Generally, delays in control processes resulting from the use of the system of IGBT transistors controlled by PWM signals have two components. The first one follows from the execution frequency of the processor/microcontroller program that manages the control loops calculating momentary duty cycles of signals governing transistor gates, and this corresponds to the abovementioned switching frequency f_s of the voltage supplied to the motor, equal to 16 kHz. Then, such a delay can be estimated by means of the first-order inertial term with the time constant of $1/16 \text{ kHz} = 62.5 \mu\text{s}$. The second delay component follows from the need to introduce time retardation between turning off the conducting transistor and turning on the non-conducting transistor within every branch of the inverter. In the real control setups assumed to be applied in all presented cases of numerical simulations, this delay called “dead time” was set at $4.1 \mu\text{s}$, and then the first-order inertial term of such a time constant was used.

6. CONCLUSIONS

In the paper, the asynchronous motor was used as an actuator for the attenuation of torsional vibrations affecting the drive systems of the rotating machines. By means of both proposed active control methods, i.e. the direct torque control (DTC-

SVM) and the rotational velocity controlled torque (RVCT), steady-state and transient torsional vibrations can be effectively suppressed. The frequency control method RVCT seemed to be more efficient when the asynchronous motor with “soft” and “medium” static characteristics was applied. However, the vector DTC-SVM method worked slightly better in the case of the motor with “stiff” static characteristics. The conceptually advanced DTC-SVM method operates faster over time and responds more smoothly when turned on and off. This is evidenced by lower instantaneous values of dynamic and electrical responses of the tested electromechanical systems. On the other hand, the frequency control method RVCT is much simpler, because it needs only one sensor measuring the driven object rotational speed and operates with constant supply voltage. However, the DTC-SVM control system, operating with variable supply voltage, must be additionally equipped with the voltage and stator phase currents measurement devices, motor torque and flux estimators as well as motor torque and flux PI controllers. Such a complex structure of this system is much more expensive, fault sensitive, and careful maintenance demanding. Moreover, as can be seen from the comparison, the RVCT method does not consume, on average, more electrical power than the vector control method DTC-SVM. Thus, it seems to be more robust and cheaper to operate, which makes this method very convenient for numerous industrial applications.

In conclusion, it is worth noting that the computational results described above made it possible to precisely determine parameters of the measurement and control equipment of the laboratory rotor drive system which was tested theoretically in this paper. Owing to this, preliminary results of an experimental verification of the computational results presented above are very promising, which will be the subject of a separate work in the near future. It should be emphasized that although the traditional DTC-SVM method has already been verified in various ways to attenuate torsional transient vibrations and ensure precision of motion parameters of drive systems, in the case of suppression of steady-state resonant vibrations considered in this paper, the firmness of the conclusions regarding the comparison of the results obtained by means of the two compared methods of asynchronous motor control can be verified using the planned experiments mentioned above.

ACKNOWLEDGEMENTS

This work was created as part of the execution of the 3rd Edition of the Program of the Polish Ministry of Education and Science “Implementation Doctorate”.

REFERENCES

- [1] E.J. Nestorides. *A Handbook on Torsional Vibration*. B.I.C.E.R.A.: Cambridge University Press, 1958.
- [2] A. Laschet. *Simulation von Antriebssystemen*. Berlin, London, New York: Springer-Verlag, 1988.
- [3] P.M. Przybyłowicz, “Torsional vibration control by active piezoelectric system,” *J. Theor. Appl. Mech.*, vol. 33, no. 4, pp. 809–823, 1995.

- [4] B.F. Spencer Jr., S.J. Dyke, M.K. Sain, and J.D. Carlson, "Phenomenological model for magnetorheological dampers". *J. Eng. Mech.*, vol. 123, no. 3, pp. 230–238, 1997, doi: [10.1061/\(ASCE\)0733-9399\(1997\)123:3\(230\)](https://doi.org/10.1061/(ASCE)0733-9399(1997)123:3(230)).
- [5] J. Wang and G. Meng, "Study of the vibration control of a rotor system using a magnetorheological fluid damper," *J. Vib. Control*, vol. 11, no. 2, pp. 263–276, 2005, doi: [10.1177/1077546305049481](https://doi.org/10.1177/1077546305049481).
- [6] A. Pęgowska, R. Konowrocki, and T. Szolc, "On the semi-active control method for torsional vibrations in electro-mechanical systems by means of rotary actuators with a magneto-rheological fluid," *J. Theor. Appl. Mech.*, vol. 51, no. 4, pp. 979–992, 2013.
- [7] T. Szolc, A. Pochanke, R. Konowrocki, and D. Pisarski, "Suppression and control of torsional vibrations of the turbo-generator shaft-lines using rotary magneto-rheological dampers," in *Proc. 12th Virtual Conference on Vibrations in Rotating Machinery (VIRM)*, Great Britain, 2020, pp. 201–211.
- [8] A. Bisoi, R. Bhattacharyya, and A.K. Samantaray, "Speed control of 3-phase induction motor in presence of Sommerfeld effect," in: *Advances in mechanism design II*, Beran, J., Bílek, M., and Žabka, P., Eds., Springer International Publishing, Cham, 2017, pp. 169–176, doi: [10.1007/978-3-319-44087-3_22](https://doi.org/10.1007/978-3-319-44087-3_22).
- [9] S.K. Bharti and A.K. Samantaray, "Resonant capture and Sommerfeld effect due to torsional vibrations in a double Cardan joint driveline," *Commun. Nonlinear Sci. Numer. Simul.*, vol. 97, p. 105728, 2021, doi: [10.1016/j.cnsns.2021.105728](https://doi.org/10.1016/j.cnsns.2021.105728).
- [10] I. Takahashi and T. Noguchi, "A new quick-response and high-efficiency control strategy of an induction motor," *IEEE Trans. Ind. Appl.*, vol. 1A-22, no. 5, pp. 820–827, 1986, doi: [10.1109/TIA.1986.4504799](https://doi.org/10.1109/TIA.1986.4504799).
- [11] Y. Xue, X. Xu, T.G. Habetler, and D.M. Divan, "A low cost stator flux oriented voltage source variable speed drive," *Conference Record of the 1990 IEEE Industry Applications Society Annual Meeting*, USA, 1990, vol.1, pp. 410–415, doi: [10.1109/IAS.1990.152218](https://doi.org/10.1109/IAS.1990.152218).
- [12] G.S. Buja and M.P. Kazmierkowski, "Direct torque control of PWM inverter-fed AC motors – a survey," *IEEE Trans. Ind. Electron.*, vol. 51, no. 4, pp. 744–757, 2004, doi: [10.1109/TIE.2004.831717](https://doi.org/10.1109/TIE.2004.831717).
- [13] T.P. Holopainen, P. Jörg, J. Niiranen, and D. Andreo, "Electric motors and drives in torsional vibration analysis and design," in *Proc. of Forty-Second Turbomachinery Symposium*, USA, October 1–3, 2013.
- [14] A. Arkkio and T.P. Holopainen, "Space-vector models for torsional vibration of cage induction motors," in *Proc. 18th International Conference on Electrical Machines and Systems (ICEMS)*, Thailand, October 25–28, 2015, pp. 1956–1962.
- [15] F. Wang, Z. Zhang, X. Mei, J. Rodríguez, and R. Kennel, "Advanced control strategies of induction machine: Field Oriented Control, Direct Torque Control and Model Predictive Control," *Energies*, vol. 11, p. 120, 2018, doi: [10.3390/en11010120](https://doi.org/10.3390/en11010120).
- [16] T. Szolc, R. Konowrocki, D. Pisarski, and A. Pochanke, "Influence of various control strategies on transient torsional vibrations of rotor-machines driven by asynchronous motors," in *Proc. 10th IFToMM International Conference on Rotor Dynamics*, "Mechanisms and Machine Science," Springer International Publishing, vol. 63, no.4, 2018; pp. 205–220, doi: [10.1007/978-3-319-99272-3_15](https://doi.org/10.1007/978-3-319-99272-3_15).
- [17] M.M. Alshbib, M.M. Elgbaily, I.M. Alsofyani, and F. Anayi, "Performance enhancement of direct torque and rotor flux control (DTRFC) of a three-phase induction motor over the entire speed range: Experimental validation," *Machines*, vol. 11, p. 22, 2023, doi: [10.3390/machines11010022](https://doi.org/10.3390/machines11010022).
- [18] T. Szolc, R. Konowrocki, M. Michajłow, and A. Pęgowska, "An investigation of the dynamic electromechanical coupling effects in machine drive systems driven by asynchronous motors," *Mech. Syst. Signal Proc.*, vol. 49, pp. 118–134, 2014, doi: [10.1016/j.ymsp.2014.04.004](https://doi.org/10.1016/j.ymsp.2014.04.004).
- [19] T. Szolc, "On the discrete-continuous modeling of rotor systems for the analysis of coupled lateral-torsional vibrations," *Int. J. Rotating Mach.*, vol. 6, no. 2, pp. 135–149, 2000, doi: [10.1155/S1023621X00000130](https://doi.org/10.1155/S1023621X00000130).
- [20] *Park, Inverse Park and Clarke, Inverse Clarke Transformations MSS Software Implementation*, User Guide, Microsemi Corporation. 2013, 50200359-0/11.13. [Online]. Available: https://www.microsemi.com/document-portal/doc_view/132799-park-inverse-park-and-clarke-inverse-clarke-transformations-mss-software-implementation-user-guide
- [21] D. Bellan, "Clarke transformation solution of asymmetrical transients in three-phase circuits," *Energies*, vol. 13, p. 5231, 2020, doi: [10.3390/en13195231](https://doi.org/10.3390/en13195231).
- [22] X. Chen, H. Wei, T. Deng, Z. He, and S. Zhao, "Investigation of electromechanical coupling torsional vibration and stability in a high-speed permanent magnet synchronous motor driven system," *Appl. Math. Model.*, vol. 64, pp. 235–248, 2018, doi: [10.1016/j.apm.2018.07.030](https://doi.org/10.1016/j.apm.2018.07.030).
- [23] H. Akagi, Y. Kanazawa, and A. Nabae., "Generalized theory of the instantaneous reactive power in the tree-phase circuits," in *Proc. IEEE International Power Electronic Conference (IPEC'83)*, 1983, pp. 1375–1386, doi: [10.1002/eej.4391030409](https://doi.org/10.1002/eej.4391030409).